J|A|C|S
ARTICLES
Published on Web 04/12/2002

Laser Flash Photolysis Kinetic Studies of Enol Ether Radical Cations. Rate Constants for Heterolysis of α-Methoxy-β-phosphatoxyalkyl Radicals and for Cyclizations of Enol Ether Radical Cations

John H. Horner,* Elsa Taxil, and Martin Newcomb*

Contribution from the Department of Chemistry, University of Illinois at Chicago, 845 West Taylor Street, Chicago, Illinois 60607

Received December 11, 2001

Abstract: Two series of enol ether radical cations were studied by laser flash photolysis methods. The radical cations were produced by heterolyses of the phosphate groups from the corresponding α-methoxy-β-diethylphosphatoxy or β-diphenylphosphatoxy radicals that were produced by 355 nm photolysis of *N*-hydroxypryidine-2-thione (PTOC) ester radical precursors. Syntheses of the radical precursors are described. Cyclizations of enol ether radical cations **1** gave distonic radical cations containing the diphenylalkyl radical, whereas cyclizations of enol ether radical cations **2** gave distonic radical cation products containing a diphenylcyclopropylcarbinyl radical moiety that rapidly ring-opened to a diphenylalkyl radical product. For 5-*exo* cyclizations, the heterolysis reactions were rate limiting, whereas for 6-*exo* and 7-*exo* cyclizations, the heterolyses were fast and the cyclizations were rate limiting. Rate constants were measured in acetonitrile and in acetonitrile solutions containing 2,2,2-trifluoroethanol, and several Arrhenius functions were determined. The heterolysis reactions showed a strong solvent polarity effect, whereas the cyclization reactions that gave distonic radical cation products did not. Recombination reactions or deprotonations of the radical cation within the first-formed ion pair compete with diffusive escape of the ions, and the yields of distonic radical cation products were a function of solvent polarity and increased in more polar solvent mixtures. The 5-*exo* cyclizations were fast enough to compete efficiently with other reactions within the ion pair ($k \approx 2 \times 10^9$ s^{-1} at 20 °C). The 6-*exo* cyclization reactions of the enol ether radical cations are 100 times faster (radical cations **1**) and 10 000 times faster (radical cations **2**) than cyclizations of the corresponding radicals ($k \approx 4 \times 10^7$ s^{-1} at 20 °C). Second-order rate constants were determined for reactions of one enol ether radical cation with water and with methanol; the rate constants at ambient temperature are 1.1×10^6 and 1.4×10^6 M^{-1} s^{-1}, respectively.

Enol ether radical cations are among the simplest members of the radical cation family, and they are readily produced in chemical or electrochemical oxidations of closed-shell enol ethers. These intermediates also are produced in non-oxidative reactions involving heterolytic fragmentation of an α-alkoxy radical containing a β-leaving group (Scheme 1). Radical heterolyses, producing radical cations and anions,[1,2] are implicated in DNA degradation reactions where a C4′ sugar radical eliminates phosphate to give an enol ether radical cation[3] that can oxidize guanosine, and this entry to DNA radicals was used by Giese's group in studies of electron (or hole) transfer in DNA.[4] The radical heterolysis entry to radical cations also has good synthetic potential because it permits formation of intermediates that are highly reactive in radical-like reactions without exposing other sensitive groups in a molecule to oxidative conditions.[5,6] Despite the biochemical and potential synthetic relevance of enol ether radical cations, however, reactions of these species are poorly understood in terms of both the mechanisms and kinetics of their reactions.[7]

Scheme 1

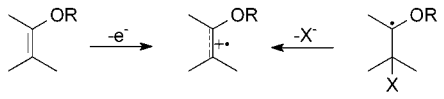

The lack of kinetic information for enol ether radical cations in general and the absence of calibrated reactions that can be used in competition kinetic experiments[8] requires that kinetics be determined directly, but direct UV monitoring is difficult because the chromophores of simple enol ether radical cations are far into the UV with λ_{max} near 200 nm.[7] In such a situation, one can use a reporter (or probe) reaction wherein a detectable

* Corresponding author. E-mail: men@uic.edu.

(1) Behrens, G.; Bothe, E.; Eibenberger, J.; Koltzenburg, G.; Schulte-Frohlinde, D. *Angew. Chem.* **1978**, *90*, 639.
(2) Gilbert, B. C.; Norman, R. O. C.; Williams, P. S. *J. Chem. Soc., Perkin Trans. 2* **1980**, 647−656.
(3) Steenken, S.; Behrens, G.; Schulte-Frohlinde, D. *Int. J. Radiat. Biol.* **1974**, *25*, 205−210.
(4) Giese, B. *Acc. Chem. Res.* **2000**, *33*, 631−636.
(5) Crich, D.; Huang, X. H.; Newcomb, M. *J. Org. Chem.* **2000**, *65*, 523−529.
(6) Crich, D.; Ranganathan, K.; Huang, X. H. *Org. Lett.* **2001**, *3*, 1917−1919.
(7) Bernhard, K.; Geimer, J.; Canle-Lopez, M.; Reynisson, J.; Beckert, D.; Gleiter, R.; Steenken, S. *Chem. Eur. J.* **2001**, *7*, 4640−4650.
(8) Newcomb, M. *Tetrahedron* **1993**, *49*, 1151−1176.

10.1021/ja0177399 CCC: $22.00

Scheme 2

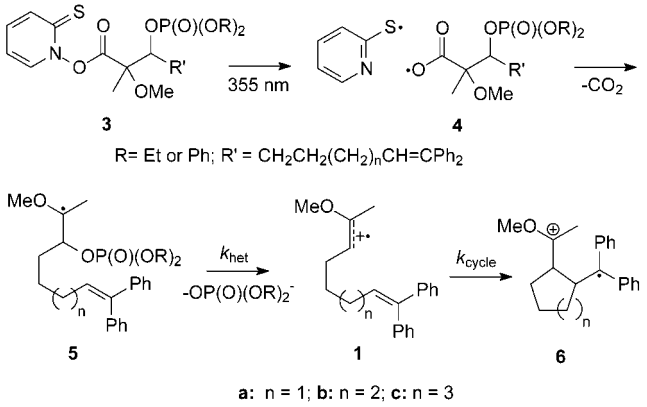

product is formed in competition with the reaction that is being measured, and the desired kinetics are extracted from the sum of the rate constants for both processes. Probe reactions for reactive transients often are bimolecular processes, and a bimolecular protocol for enol ether radical cation detection was reported.[9] In this work, we describe the preparation and kinetic studies of unimolecular enol ether radical cation reporter reactions that were developed for applications in laser flash photolysis (LFP) kinetic methods.[10,11] The unimolecular approach offers advantages in terms of the reproducibility of the reporter reaction kinetics and in the broad scope of reactions that can be studied, and our results also provide information about the processes occurring in the ion pair produced in the radical heterolysis reactions.

Results

The experimental requirements for enol ether radical cation clocks for LFP applications are that the radical cations are produced efficiently and that the reporter reaction provides a readily detectable signal. Desirable, but not requisite, properties are that the initial reactions giving the radical cation clocks are fast and that a method for determining yields exists. We were able to incorporate all of these properties into the clocks by using *N*-hydroxypyridine-2-thione (PTOC) ester[12] precursors to α-alkoxy radicals that contain *β*-phosphate leaving groups. We designed two series of clocks (**1**, **2**) that ultimately produce diphenylalkyl radicals that contain a strong long-wavelength chromophore centered in the range 330−335 nm.

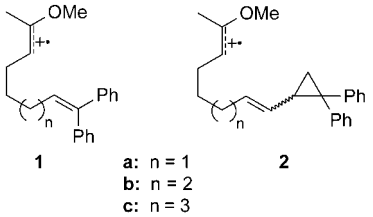

The reaction sequence for radical cations **1** is shown in Scheme 2. Laser flash photolysis (LFP) of the PTOC esters **3** gave acyloxyl radicals **4** that decarboxylated "instantly" on the nanosecond time scale to give the α-methoxy-*β*-phosphatoxy radicals **5**. Heterolytic fragmentation of the phosphate groups in radicals **5** gave radical cations **1**. Cyclization of radical cations **1** gave the distonic radical cations **6** that were detected at 330−335 nm. Radical cations **1a** and **1b** were produced from both *β*-diethylphosphatoxy and *β*-diphenylphosphatoxy radicals, and radical cation **1c** was produced from the *β*-diphenylphosphatoxy radical. The leaving group can have an effect on the kinetics and yields of products, and we used a labeling that identifies the phosphate group. For example, radical **5b-E** is the *β*-diethyl phosphate radical that gives radical cation **1b**, whereas radical **5b-P** is the *β*-diphenyl phosphate radical that gives the same radical cation, **1b**.

Scheme 3

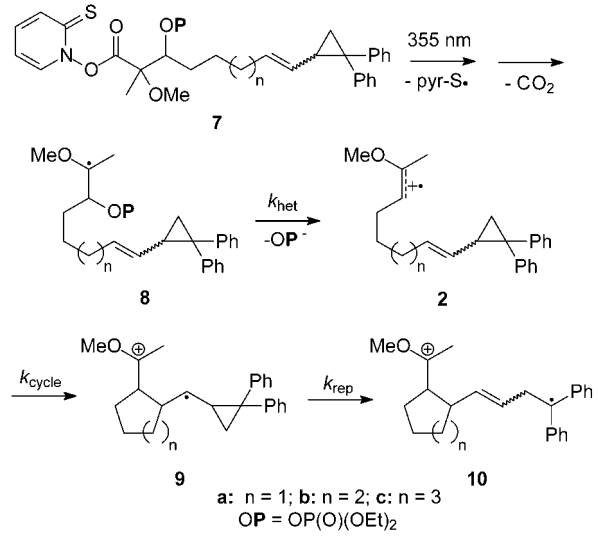

Scheme 4 [a]

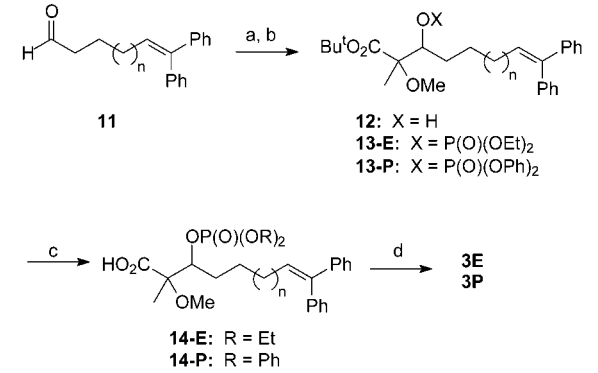

[a] Key: (a) *t*-$BuO_2CCH(OMe)CH_3$, LDA. (b) $(RO)_2P(O)Cl$. (c) TFA, CH_2Cl_2. (d) 2,2′-Dipyridyl disulfide bis-*N*-oxide, Bu_3P.

The reaction sequence for radical cations **2** (Scheme 3) is similar to that for radical cations **1**. The difference in this sequence is that distonic radical cations **9**, formed by cyclizations of **2**, further react by cyclopropylcarbinyl radical ring openings to give the detectable diphenylalkyl radicals **10**. We used *β*-diethyl phosphate radicals as the precursors to radical cations **2** because the synthetic route to the *β*-diphenyl phosphate precursors was precluded (see below).

Preparation of Precursors. The synthetic sequence for the precursors to radicals **1** is shown in Scheme 4. Hydroxyalkylation of the enolate from the *tert*-butyl ester of 2-methoxypropanoic acid with the known aldehydes **11** gave α-methoxy-*β*-hydroxy esters **12** that were not isolated but were phosphorylated with either diethyl- or diphenylphosphoryl chloride

(9) Newcomb, M.; Miranda, N.; Huang, X. H.; Crich, D. *J. Am. Chem. Soc.* **2000**, *122*, 6128−6129.
(10) A portion of this work has been communicated. See ref 11.
(11) Horner, J. H.; Newcomb, M. *J. Am. Chem. Soc.* **2001**, *123*, 4364−4365.
(12) Barton, D. H. R.; Crich, D.; Motherwell, W. B. *Tetrahedron* **1985**, *41*, 3901−3924.

Scheme 5 [a]

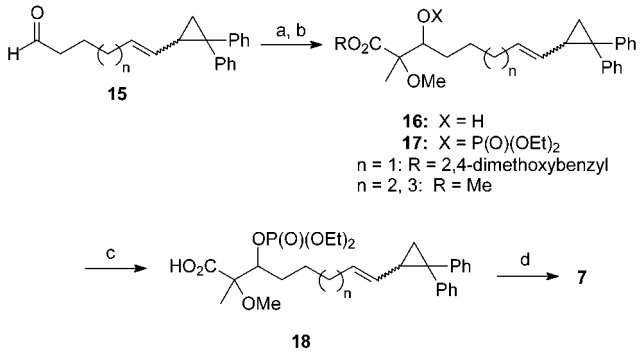

[a] Key: (a) $RO_2CCH(OMe)CH_3$, LDA. (b) $(EtO)_2P(O)Cl$. (c) NaOH or KOH, EtOH, H_2O. (d) 2,2′-Dipyridyl disulfide bis-*N*-oxide, Bu_3P.

to give phosphates **13-E** and **13-P**, respectively. In each case, one diastereomer of **13** was obtained by column chromatography. We assign (2*RS*,3*RS*) stereochemistry to the major diastereomer on the basis of the analogous reactions reported by Heathcock,[13] but the stereochemistry was not further studied because it is not important; a chiral center is lost in formation of the radical, giving the same product radical from each diastereomer. The esters were converted to the parent carboxylic acids **14** by reaction with TFA. Acids **14** were then converted to the PTOC esters **3** by conventional methods.

The synthetic sequence for the precursors to radical cations **2** (Scheme 5) was similar to that employed for the precursors to **1**. The intermediate methyl esters or 2,4-dimethoxybenzyl esters **17** were saponified to give the β-diethyl phosphate carboxylic acids **18**. We were not able to prepare β-diphenyl phosphate precursors to radical cations **2**. The β-diphenyl phosphates were not stable to basic saponification conditions and, thus, required TFA hydrolysis of *tert*-butyl esters, but the vinylcyclopropane moiety in these compounds was not stable to TFA treatment.

Spectra and Yields. Figure 1A shows a time-resolved spectrum after laser irradiation of PTOC ester **3b-E** (precursor to radical cation **1b**) that is representative of the spectra from reactions of radical cations **1**. The signal growing in with λ_{max} at 332 nm is from the diphenylalkyl radical **6b**, and the position of the absorbance is similar to that of the diphenylmethyl radical.[14] The bleaching centered at 360 nm is from destruction of the PTOC ester precursor. The absorbance centered at 490 nm is from the byproduct of the photolysis reaction, the pyridine-2-thiyl radical for which the molar extinction coefficient has been reported.[15] Figure 1B shows the time-resolved spectrum following photolysis of PTOC ester **7b** (precursor to radical cation **2b**) that has the same features as above, in this case, from the final product, distonic radical cation **10b**.

The insets in Figure 1 show kinetic traces recorded at 335 and 490 nm. The initial intensity of the 490 nm signal from the pyridine-2-thiyl radical was used as a standard for measuring the ultimate yields of diphenylalkyl radicals formed from radicals **1** and **2**. We used molar extinction coefficients of $\epsilon =$ 3 200 for the pyridine-2-thiyl radical[15] and $\epsilon =$ 20 000 for the diphenylalkyl radicals. An internal check on the relative extinction coefficients was possible because, in several cases, the yields of diphenylalkyl radicals reached values close to 100% in high polarity solvent.

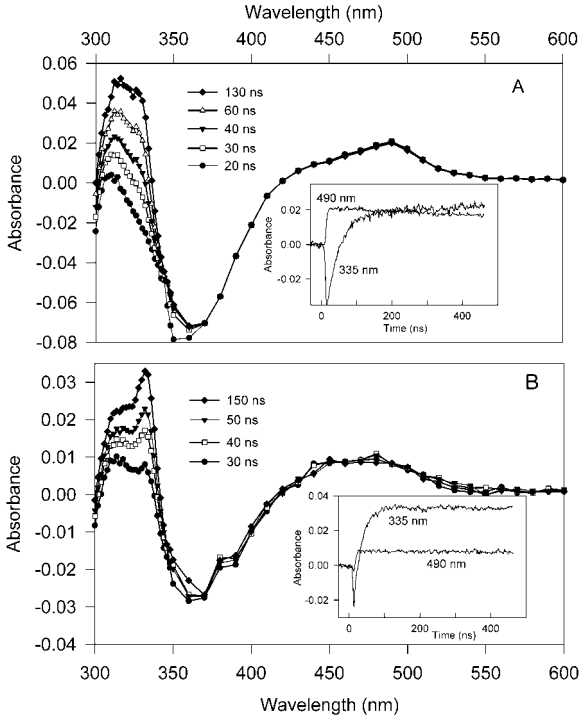

Figure 1. Time-resolved spectra from reactions of radicals **1b** (A) and **2b** (B). The bleachings centered at 360 nm are from destruction of the PTOC ester precursors. The insets show the kinetic traces at 335 (λ_{max} for diphenylalkyl radicals) and 490 nm (λ_{max} for the 2-pyridinethiyl radical).

Table 1. Percent Yields of Product Distonic Radical Cations **6** and **10**[a]

radical	ACN[b]	0.5% TFE[c]	1.0% TFE[c]	2.5% TFE[c]
5a-E	50	44	65	92
5a-P[c]	85	98	100	100
8a	65	80		95
5b-E	14	42	65	70
5b-P	34	61	80	80
8b	25	80	90	100
5c-P	12	22	47	60
8c			10	20

[a] Yields of products **6** and **10** determined by comparison of the ultimate diphenylalkyl radical absorbance to the initial thiopyridyl radical absorbance. The estimated accuracy is ±10% of the value given. [b] ACN = acetonitrile. [c] TFE = 2,2,2-trifluoroethanol. The percentage of TFE in ACN is listed. [c] 15% yield observed in THF.

Table 1 lists the yields of distonic radical cations **6** and **10** as a function of solvent. Because the leaving group has an influence on the yields, we identified the specific β-phosphatoxyalkyl radicals that were produced in the initial photolysis reactions. Reactions were conducted in acetonitrile (ACN) and in ACN solutions containing 2,2,2-trifluoroethanol (TFE). A solvent polarity effect was apparent with yields consistently increasing for all radical cations when the solvent polarity was increased. Figure 2 shows the effect for radical **5b-E** that is especially dramatic. A leaving group effect also was apparent in that the product yields from the diphenylphosphatoxy radicals **5a-P** and **5b-P** were consistently greater than those from the diethylphosphatoxy radicals **5a-E** and **5b-E**, respectively, even though the same radical cations (**1a** and **1b**, respectively) were formed from these pairs. As discussed later, the reduced yields

(13) Heathcock, C. H.; Pirrung, M. C.; Young, S. D.; Hagen, J. P.; Jarvi, E. T.; Badertscher, U.; Märki, H.-P.; Montgomery, S. H. *J. Am. Chem. Soc.* **1984**, *106*, 8161−8174.
(14) Chatgilialoglu, C. In *Handbook of Organic Photochemistry*; Scaiano, J. C., Ed.; CRC Press: Boca Raton, FL, 1989; Vol. 2, pp 3−11.
(15) Alam, M. M.; Watanabe, A.; Ito, O. *J. Org. Chem.* **1995**, *60*, 3440−3444.

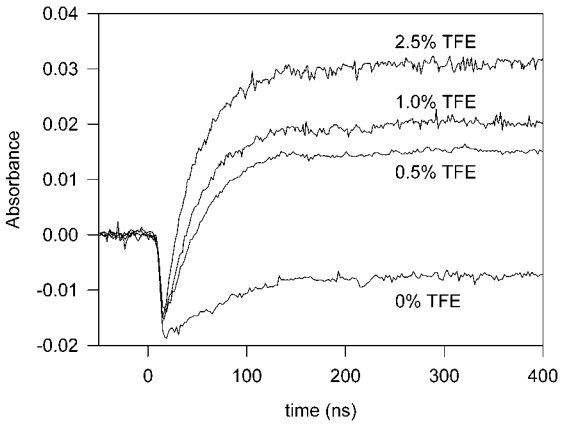

Figure 2. Kinetic traces at 330 nm for reaction of radical **5b-P** in acetonitrile containing 2,2,2-trifluoroethanol in the amounts shown on the labels. In each case, the 330 nm signal was normalized against the intensity of the 490 nm signal (from the pyridine-2-thiyl radical) obtained in the same experiment.

in the lower polarity solvents must be due to reactions of the first-formed radical cation with the phosphate anion in the ion pair produced in the heterolysis reaction.

The greatest yield of distonic radical cation product found in ACN containing no TFE was formation of **6a** in 85% yield from reaction of radical **5a-P**. When the reaction of **5a-P** was conducted in the lower polarity solvent THF, the yield of **6a** was reduced to about 15%. In discussion, we will argue that diffusive escape from the initially formed ion pair most likely does not occur in THF, and the yield of distonic radical cation **6a** reflects competition within the ion pair between cyclization of the radical cation **1a** and reactions that consume it.

Kinetics. In the sequences of reactions shown in Schemes 2 and 3, the initial photolytic cleavages and the subsequent decarboxylation reactions are faster than the temporal resolution of the nanosecond kinetic spectrometer. In the case of radicals **2**, the ring opening "reporter" reactions of distonic radical cations **9** have rate constants (k_{rep}) of about 4×10^{11} s^{-1} at ambient temperature.[16] Therefore, the "slow" reactions for which kinetics are obtained in both series of radical cations **1** and **2** are the heterolysis reactions of the α-methoxy-β-phosphatoxyalkyl radicals **5** and **8** (k_{het}) that produce the enol ether radical cations, the cyclizations of radical cations **1** and **2** to distonic radical cations **6** and **10**, respectively, (k_{cycle}) or a convolution of these processes.

LFP kinetic studies were performed in ACN and in solutions of ACN containing TFE. Arrhenius functions were determined for several cases (Figure 3 and Table 2). Table 3 contains rate constants at ambient temperature. For cases where Arrhenius functions were determined, the rate constants in Table 3 are those calculated for 20 °C from the Arrhenius function; for other cases, the kinetic values are those measured at (20.0 ± 0.2) °C.

As developed in the Discussion, the rate-limiting processes for radical cations **1a** and **2a** were the heterolysis steps, whereas the 6-*exo* and 7-*exo* cyclization reactions were the rate-limiting processes for radical cations **1b**, **2b**, **1c**, and **2c** in ACN containing TFE. For radical **8b** at low reaction temperatures, the kinetic traces showed a convolution of two processes (Figure 4), and the kinetics of each were obtained by deconvolution

(16) Newcomb, M.; Johnson, C. C.; Manek, M. B.; Varick, T. R. *J. Am. Chem. Soc.* **1992**, *114*, 10915−10921.

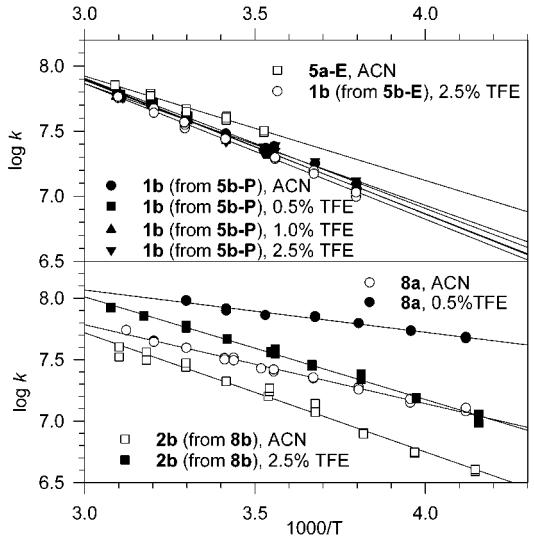

Figure 3. Arrhenius functions for reactions determined in this work. The reactions of radicals **5a-E** and **8a** involve rate-limiting heterolyses, whereas the reactions of radical cations **1b** and **2b** involve rate-limiting cyclization.

Table 2. Arrhenius Functions for Reactions of Radicals **5** and **8**

radical	solvent[a]	Arrhenius function[b]	temp range[c]
		rate-limiting heterolysis reactions	
5a-E	ACN	$(10.32 \pm 0.22) - (3.66 \pm 0.30)/\theta$	10 to 51
8a	ACN	$(9.71 \pm 0.10) - (2.94 \pm 0.12)/\theta$	−30 to 47
	0.5% TFE	$(9.10 \pm 0.11) - (1.57 \pm 0.14)/\theta$	−30 to 30
		rate-limiting cyclization reactions	
1b (from **5b-E**)	ACN[d]	$(9.9 \pm 0.5) - (3.7 \pm 0.6)/\theta$	20 to 51
	2.5% TFE	$(10.99 \pm 0.14) - (4.76 \pm 0.19)/\theta$	−10 to 50
1b (from **5b-P**)	ACN	$(10.90 \pm 0.17) - (4.57 \pm 0.23)/\theta$	−10 to 50
	0.5% TFE	$(11.03 \pm 0.36) - (4.77 \pm 0.50)/\theta$	10 to 49
	1.0% TFE	$(10.96 \pm 0.32) - (4.69 \pm 0.45)/\theta$	10 to 50
	2.5% TFE	$(10.68 \pm 0.25) - (4.29 \pm 0.33)/\theta$	−10 to 50
2b (from **8b**)	ACN[e]	$(10.47 \pm 0.17) - (4.23 \pm 0.21)/\theta$	−32 to 50
	2.5% TFE	$(10.52 \pm 0.12) - (3.82 \pm 0.15)/\theta$	−32 to 52

[a] ACN = acetonitrile; TFE = 2,2,2-trifluoroethanol. The percentage of TFE in ACN is listed. [b] Errors given at 2σ. $\theta = 2.303RT$ in kcal/mol. [c] Temperature range studied in °C. [d] Undeconvoluted data; the heterolysis and cyclization reactions have similar rate constants. [e] Data deconvoluted to correct for slow heterolysis; the rate constants are for the cyclization reaction.

Table 3. Rate Constants for Reactions of Radicals **5** and **8** at Ambient Temperature[a]

radical	ACN[b]	0.5% TFE[b]	1.0% TFE[b]	2.5% TFE[b]
5a-E	$\mathbf{3.9 \times 10^7}$	8×10^7	1.1×10^8	$>2 \times 10^8$
5a-P[c]	$>2 \times 10^8$	$>2 \times 10^8$	$>2 \times 10^8$	$>2 \times 10^8$
8a	$\mathbf{3.3 \times 10^7}$	$\mathbf{8.5 \times 10^7}$		$>2 \times 10^8$
5b-E	$\mathbf{1.4 \times 10^7}$	2.4×10^7	2.6×10^7	$\mathbf{2.7 \times 10^7}$
5b-P	$\mathbf{3.1 \times 10^7}$	$\mathbf{3.0 \times 10^7}$	$\mathbf{2.9 \times 10^7}$	$\mathbf{3.0 \times 10^7}$
8b	$\mathbf{2.1 \times 10^7}$	3.9×10^7	4.5×10^7	$\mathbf{4.7 \times 10^7}$
5c-P	3.5×10^5	2.8×10^5	1.4×10^5	1.2×10^5
8c			2×10^5	1×10^5

[a] In units of s^{-1}. Values in bold face are rate constants at 20 °C calculated from the Arrhenius functions in Table 2. Other rate constants are measured values in the range (20 ± 0.2) °C. The instrumental limit is 2×10^8 s^{-1}. [b] ACN = acetonitrile; TFE = 2,2,2-trifluoroethanol. The percentage of TFE in ACN is listed. [c] Rate constant in THF $>2 \times 10^8$ s^{-1}.

(data are given in the Supporting Information). The Arrhenius function and rate constant reported for this radical in Tables 2 and 3 are for the 6-*exo* cyclization reaction. Convolution of the heterolysis and cyclization kinetics was expected for radical **5b-E** reacting in ACN as discussed later, but due to the low

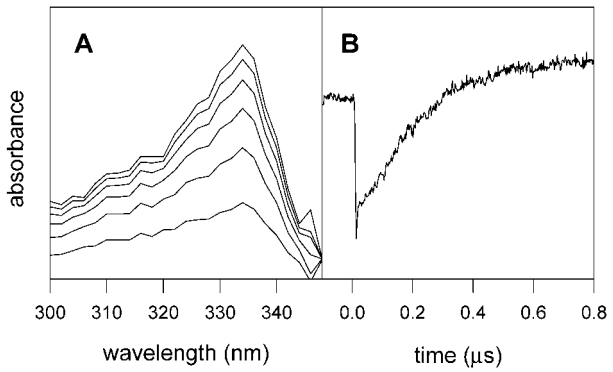

Figure 4. (A) Time-resolved growth spectrum at 20 ns intervals from 61 ns after photolysis of PTOC ester **7b** in acetonitrile at 21 °C. The spectral trace at 41 ns was subtracted from each spectrum to give a zero baseline. (B) Convoluted kinetic trace at 335 nm following photolysis of **7b** in acetonitrile at −20 °C. The initial bleaching is from destruction of the precursor.

yield of product radical **6b**, the signal-to-noise was not adequate for deconvolution. For this case, we report the apparent first-order rate constant of the reaction and note that this is a lower limit.

To demonstrate the use of the radical cation clocks in LFP kinetic studies, we determined rate constants for reactions of radical cation **1c** with water and with methanol at ambient temperature in acetonitrile containing 2.5% TFE. PTOC ester **3c-P** was employed as the precursor. Reactions were conducted with varying amounts of water or methanol. The observed rate constant (k_{obs}) for reaction of **1c** is given by eq 1 where k_{cycle} is the first-order rate constant for cyclization of **1c**, k_{Trap} is the second-order rate constant for reaction of the radical cation with water or methanol, and [Trap] is the concentration of water or methanol in a particular run. Assuming that the rate constant for cyclization **1c** is essentially constant over the concentration range of water or methanol employed, a plot of k_{obs} versus [Trap] will have a slope of k_{Trap}. The rate constant for reaction of water with **1c** was $(1.1 \pm 0.1) \times 10^6$ M^{-1} s^{-1}, and the rate constant for reaction of methanol with **1c** was $(1.4 \pm 0.4) \times 10^6$ M^{-1} s^{-1}. We note that these rate constants could be for reaction of water and methanol as nucleophiles, as bases that deprotonate the radical cation, or a combination of nucleophilic capture and deprotonation.

$$k_{obs} = k_{cycle} + k_{Trap}\,[Trap] \qquad (1)$$

Discussion

Rate-Limiting Reactions. A series of fast processes are involved in the reactions studied in this work (Schemes 2 and 3), but the phosphate heterolysis (k_{het}) reactions and cyclization reactions (k_{cycle}) are the "slower" processes for which rate constants were measured. The photochemical cleavages of the N−O bonds in the PTOC esters are instantaneous reactions on the nanosecond time scale, and the decarboxylation reactions of acyloxyl radicals to give alkyl radicals occur in less than 1 ns.[17] In the case of radical cations **2**, cyclopropylcarbinyl radical ring openings follow the cyclization reactions that give distonic radical cations **9**, and the ring openings of 2,2-diphenylcyclopropylcarbinyl radicals have rate constants of about 5×10^{11} s^{-1} at ambient temperature.[16]

The solvent effects on the kinetics for reactions of **5a-E** and **8a** (diethyl phosphate leaving group, 5-*exo* cyclizations) indicate that the rate-limiting processes are the heterolysis reactions. The kinetics for these two radicals are quite similar in ACN and in 0.5% TFE in ACN, and they dramatically accelerate with increasing solvent polarity such that the reactions are faster than the instrument limit in 2.5% TFE.

Radical **5a-P** gives the same radical cation as radical **5a-E** (i.e. **1a**), but for **5a-P** the kinetics for this reaction were too fast to measure in ACN demonstrating that the heterolysis, and not the cyclization step, was rate-limiting. The heterolysis reaction was still too fast to measure when radical **5a-P** was allowed to react in the low polarity solvent THF. The increased rate constant for reaction of **5a-P** in comparison to **5a-E** is consistent with the decreased basicity of the diphenyl phosphate group compared to that of the diethyl phosphate group; that is, diphenylphosphoric acid is about 1 pK_a unit more acidic than diethylphosphoric acid.[18]

The heterolysis rate constants for radicals **5a-E**, **5a-P**, and **8a** are in qualitative agreement with those found previously. In reactions of radicals **19-E** and **19-P**,[9] the enol ether radical cation produced is less stable than radical cations **1** and **2** in that it lacks one alkyl group, and the rate constants for heterolyses of radicals **19** determined by LFP studies of solutions in ACN were smaller than those found in the present work.[9] Consistent with observations here, heterolysis of radical **19-P** was considerably faster than heterolysis of **19-E**. Radical **20**, which gives an enol ether radical cation with a substitution pattern the same as **1** and **2**, was found to heterolyze in MeOH with a rate constant exceeding 3×10^9 s^{-1}.[19] We return to these kinetic values below when we discuss the multiple reactions that comprise the "heterolysis reaction".

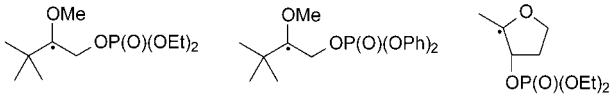

19-E **19-P** **20**

The Arrhenius log *A* terms for **5a-E** and **8a** deserve special note. If the entropy of activation were zero at 298 K, then the log *A* term would be 13.1. Fragmentation reactions can have positive entropies of activation giving log *A* values of up to 16,[20] but that would be expected for gas-phase reactions or homolytic cleavages in solution that do not produce charge. The heterolytic cleavage reactions we are studying here do create charge in the transition state, and the small log *A* terms found indicate a high degree of organization in these cleavages. Highly defined organization in the cleavage of radicals **5a** and **8a** might be required for efficient charge-stabilization in the incipient radical cations and phosphate anions, and similar log *A* terms were found for β-phosphatoxy and β-acetoxy radicals that heterolyzed to give styrene radical cations.[21−24] It is also possible

(17) Bockman, T. M.; Hubig, S. M.; Kochi, J. K. *J. Org. Chem.* **1997**, *62*, 2210−2221.
(18) Peppard, P. F.; Mason, G. W.; Andrejasich, C. M. *Inorg. Nucl. Chem.* **1965**, *27*, 697−709.
(19) Gugger, A.; Batra, R.; Rzadek, P.; Rist, G.; Giese, B. *J. Am. Chem. Soc.* **1997**, *119*, 8740−8741.
(20) Benson, S. W. *Thermochemical Kinetics*, 2nd ed.; Wiley: New York, 1976.
(21) Choi, S. Y.; Crich, D.; Horner, J. H.; Huang, X. H.; Martinez, F. N.; Newcomb, M.; Wink, D. J.; Yao, Q. W. *J. Am. Chem. Soc.* **1998**, *120*, 211−212.

that the solvent is highly organized in the TS of the heterolysis to accommodate the formation of charge.

For reactions in the "**b**" series (the 6-*exo* cyclizations of radical cations **1b** and **2b**), the cyclization reactions and not the heterolyses were rate limiting in ACN solutions containing TFE. These reactions were found to be slower than those in the "**a**" series in the same solvent mixture, and the solvent polarity effects on the kinetics were minor. The good match in the rate constants from radicals **5b-E** and **5b-P**, both of which give radical cation **1b**, demonstrates that the heterolyses steps were not involved in the kinetics.

In ACN without TFE, however, the observed rate constants for the diethyl phosphate-containing radicals **5b-E** and **8b** were convolutions of the rate constants for heterolysis and cyclization. The diphenylphosphatoxy radical **5b-P** in ACN must heterolyze much faster than the measured rate by analogy to radical **5a-P**, and the observed rate constant for **5b-P** in ACN is that for the cyclization of radical cation **1b**. In the case of radical **8b** reacting to give radical cation **2b**, we could deconvolute the two rate constants, but this was not possible for radical **5b-E** because the yield was low, and the signal-to-noise was poor. Thus, the reported kinetic values for **5b-E** in ACN are from first-order solutions to data that are convoluted. Because the convolution of similar rate constants results in an apparent first-order rate constant that is smaller than the actual values, the reported rate constant for "cyclization" of radical **1b** in ACN of 1.4×10^7 s^{-1} at 20 °C is a lower limit; the actual value will be close to 2×10^7 s^{-1}.[25]

The Arrhenius parameters for the reactions in the "**b**" series are consistent with those expected for 6-*exo* cyclizations if one uses the results of radical cyclizations as a guide. Specifically, the entropic terms (log *A*) for cyclizations of **1b** and **2b** are quite similar to those for analogous carbon-centered radicals.[8,26,27] It is perhaps more interesting to focus on the activation energies for these cyclization reactions that are the key features in the kinetics. The enol ether radical cation cyclizations were expected to be much faster than the cyclizations of analogous radicals, and that is the case for radicals **1b** and **2b**, which cyclize at ambient temperature about 100 and 10 000 times faster than radicals **21** and **22**, respectively.[27,28] If one considers the cyclization reaction to be a typical "radical reaction", the radical cations might be regarded as super-radicals.

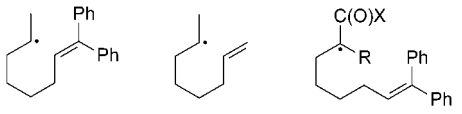

21 **22** **23a:** R = H **23b:** R = Me

One surprising kinetic result is that radical cations **1b** and **2b** have comparable rate constants for cyclization, unlike the case of alkyl radicals **21** and **22** where the diphenylethene moiety in **21** results in about a 100-fold increase in the rate of cyclization in comparison to **22**. The origin of this effect is not apparent, but it clearly is not a result of an offset between activation energies and entropies of activation for the cyclizations. One possible explanation is that the diphenylethenyl group inherently accelerates the cyclization by providing a more stable radical product as it does for simple radical cyclizations, but a steric interaction of the highly substituted radical cation center with this moiety works to retard the cyclization. Some support for this conjecture is found in the cyclizations of tertiary α-ester and α-amide radicals **23b** that are 2 orders of magnitude slower than cyclizations of the analogous secondary radicals **23a**, apparently due to steric effects involving the planar radical center.[26,29]

Only limiting values could be obtained for the kinetics of the 7-*exo* cyclizations of enol ether radical cations **1c** and **2c** because these cyclization reactions were slow enough such that bimolecular reactions were important in the overall rates of reaction. Competing reactions are indicated for radical cation **2c** by the low yields of product **10c** and the fact that the observed rate constants *increased* when the reactions were conducted with increasingly dilute solutions (data not shown). The yields of distonic radical cation product **6c** from radical cation **1c** are similar to the product yields from radical cation **1b** produced from the phosphate radical precursor **5b-P**, but the observed decrease in rate constants as the solvent polarity was increased suggests that second-order reactions of **1c** with phosphate anion are increasingly important in the lower polarity solvent mixtures. Because the observed rate constant is the sum of all rate constants for reactions of **1c**, the values we obtained must be upper limits for the rate constants for cyclizations.

Ion-Pair Reactions. The ultimate yields of diphenylalkyl radical products **6** and **10** provide information about reactions occurring in the ion pairs initially produced by the heterolysis reactions. The 6-*exo* cyclizations of **1b** and **2b** were slow enough such that cyclization occurred for diffusively free radical cations only (see above). If one focuses on the yields of products from the 6-*exo* cyclization reactions in Table 1, one sees that the yields appreciably increased as the solvent polarity increased by addition of TFE. This solvent polarity effect on yield reflects increasing amounts of radical cation that successfully escape from the initially formed ion pairs as the solvent polarity was increased.

Scheme 6 shows the possible reactions in the ion pair. The initial heterolysis reaction produces an ion pair with a dialkyl phosphate anion positioned next to the enol ether radical cation. Collapse of the ion pair will return the *β*-phosphate radical or a rearranged radical **24**. If the original radical is produced in an ion pair collapse reaction, it will simply heterolyze again. Radical **24** might heterolyze back to the ion pair rapidly, but there is evidence that *β*-alkoxy-*β*-phosphatoxyalkyl radicals such as **24** will be more stable than α-alkoxy-*β*-phosphatoxyalkyl radicals. For example, computed energies for radicals **26** and **27** at the B3LYP/6-31G* level indicate that **27** is more stable than **26** by about 3 kcal/mol due to an anomeric effect that stabilizes radical **27**.[30] If radical **24** does not heterolyze rapidly,

(22) Choi, S. Y.; Crich, D.; Horner, J. H.; Huang, X. H.; Newcomb, M.; Whitted, P. O. *Tetrahedron* **1999**, *55*, 3317−3326.
(23) Whitted, P. O.; Horner, J. H.; Newcomb, M.; Huang, X. H.; Crich, D. *Org. Lett.* **1999**, *1*, 153−156.
(24) Newcomb, M.; Horner, J. H.; Whitted, P. O.; Crich, D.; Huang, X. H.; Yao, Q. W.; Zipse, H. *J. Am. Chem. Soc.* **1999**, *121*, 10685−10694.
(25) Simulated convoluted data for consecutive reactions, both with rate constants of 3×10^7 s^{-1}, give an apparent rate constant of 1.8×10^7 s^{-1} when solved as a first-order process.
(26) Newcomb, M.; Horner, J. H.; Filipkowski, M. A.; Ha, C.; Park, S. U. *J. Am. Chem. Soc.* **1995**, *117*, 3674−3684.
(27) Newcomb, M.; Choi, S. Y.; Horner, J. H. *J. Org. Chem.* **1999**, *64*, 1225−1231.
(28) Beckwith, A. L. J.; Moad, G. *J. Chem. Soc., Chem. Commun.* **1974**, 472−473.
(29) Musa, O. M.; Choi, S. Y.; Horner, J. H.; Newcomb, M. *J. Org. Chem.* **1998**, *63*, 786−793.
(30) Horner, J. H. Unpublished results.

Scheme 6

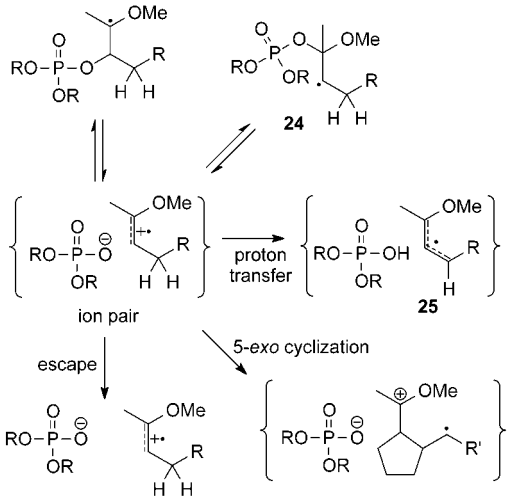

its formation will serve as a trapping reaction that leads to lower yields of detectable products because cyclization of **24** would be much too slow to be important on the time scale of the kinetic measurements.[27,28]

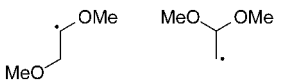

26 **27**

Alternatively, deprotonation of the radical cation by the phosphate anion within the ion pair is possible. This reaction would give allylic radical **25** and phosphoric acid, and the process will definitely lead to a reduction in yield of detected diphenylalkyl radical products. A 4-*exo* cyclization of radical **25** produced from the "**a**" series would be too slow to measure by LFP methods, and a 5-*exo* cyclization of radical **25** produced from the "**b**" series will be much slower than a conventional 5-*exo* radical cyclization, which has a rate constant of about 2×10^5 s^{-1} at 20 °C for the 5-hexenyl radical.

From the data in this work, it is not possible to identify which of the above processes is more prevalent in reducing the yields of distonic radical cation products, but previous results suggest that both reactions are likely to occur. For example, phosphate dianion in water traps enol ether radical cations to give β-alkoxy-β-phosphate radicals, and α-alkoxy-β-phosphate radicals are not detected;[7] this could be a kinetic effect, but it is possible that the latter were formed reversibly, and the former were more stable. In addition, the yields of radical cations formed from heterolyses of β-phosphate radicals **19** are lower in ACN than in ACN containing TFE, much like the solvent effect on yield seen here, but deprotonation is not possible for this system, suggesting that collapse to a less reactive β-alkoxy-β-phosphate radical occurred.[9] Deprotonation reactions of enol ether radical cations by dialkyl phosphate anions are known to occur, however.[31] The fact that the yields are more severely reduced in reactions of β-diethyl phosphate radicals than in reactions of β-diphenyl phosphate radicals appears to be more consistent with a deprotonation reaction because diethyl phosphate is a stronger base,[18] although diethyl phosphate might also react more rapidly in the nucleophilic addition reaction that gives radical **24**.

(31) Giese, B.; Beyrich-Graf, X.; Erdmann, P.; Petretta, M.; Schwitter, U. *Chem. Biol.* **1995**, *2*, 367−375.

Table 4. Normalized Relative Rate Constants for Reactions Occurring in Ion Pairs in ACN[a]

radical cation	phosphate	cyclization	deprotonation[b]	escape	D/E[c]
1b	$(EtO)_2P(O)O^-$		86	14	6.1
1b	$(PhO)_2P(O)O^-$		66	34	2.0
2b	$(EtO)_2P(O)O^-$		75	25	3.0
1a	$(EtO)_2P(O)O^-$	46	46	8	
1a	$(PhO)_2P(O)O^-$	77	15	8	
2a	$(EtO)_2P(O)O^-$	53	35	12	

[a] See discussion in text for the method. [b] Deprotonation to give allyl radical **25** and/or collapse to radical **24**. [c] Ratio of deprotonation and/or collapse in the ion pair to diffusive escape.

We thus envision two solvent polarity effects at play in the reactions we studied. Increasing solvent polarity increased the rate of heterolysis of the β-phosphate radicals as indicated in the strong polarity effect observed in the kinetics of reactions of **5a-E** and **8a**. In addition, increased solvent polarity resulted in more efficient formation of free ions, most likely by accelerating the ion pair escape reaction.

Another ion pair reaction is obviously important for the 5-*exo* cyclizations. The yields of products from these cyclizations in ACN are much greater than the yields of products from the corresponding 6-*exo* cyclizations. If our model of diffusive escape competing with reactions within the contact ion pair is correct, then the 5-*exo* cyclizations of **1a** and **2a** must compete efficiently with other reactions of the radical cation in the ion pair, thus resulting in increased yields of detectable diphenylalkyl radicals. That is, the 5-*exo* cyclizations must be occurring partially within the contact ion pair as shown in Scheme 6. We note that either deprotonation or nucleophilic capture of the distonic radical cation product *following* the cyclization in the ion pair would give products that still contain the diphenylalkyl radical moiety and will be indistinguishable by UV spectroscopy from the distonic radical cation product formed by cyclization of the diffusively free radical cation.

The relative yields for the two pairs of β-diethyl phosphate radicals (**5a-E** vs **5b-E**, and **8a** vs **8b**) and that for the β-diphenylphospate radicals (**5a-P** vs **5b-P**) can be used to establish the relative rate constants for processes occurring in the ion pair in ACN (Table 4). From the yield data for the 6-*exo* cyclizations, we established the relative rate constants for deprotonation and/or collapse to radical **24** versus diffusive escape from the ion pairs. The ratio of these rate constants (D/E) was then used to calculate the approximate amount of 5-*exo* cyclization product formed from diffusively free radical cations **1a** and **2a**. The remaining yields of cyclic product for radical cations **1a** and **2a** are ascribed to 5-*exo* cyclizations occurring in the ion pair. This crude analysis indicates that (1) deprotonation by the diethyl phosphate anion and/or collapse to radical **24** is about three times as fast as deprotonation by and/or collapse of the diphenyl phosphate anion, (2) the relative amount of diffusive escape was consistently small in ACN, and (3) the 5-*exo* cyclizations of radical cations **1a** and **2a** had similar rate constants as expected from the results of 6-*exo* cyclizations of **1b** and **2b** where cyclization rate constants were measured.

We can add a semiquantitative aspect to the analysis in Table 4 by assuming that 5-*exo* cyclizations of the radical cations **1a** and **2a** are about 50 times faster than 6-*exo* cyclizations of radical cations **2a** and **2b**; this difference in rate constants for 5-*exo* and 6-*exo* cyclizations has been found in a number of

LFP kinetic studies of radical cyclizations.[26,27,29,32−34] If that approximation holds for the enol ether radical cations, then the 5-*exo* cyclizations and deprotonation by the diethyl phosphate anion and/or ion pair collapse have rate constants at ambient temperature in the range $1-2 \times 10^9$ s^{-1}. The deprotonation by the diphenyl phosphate anion and/or ion pair collapse and diffusive escape from the ion pair have rate constants that are smaller, in the range $2-4 \times 10^8$ s^{-1}.

We note that the rate constants estimated above are for reactions in ACN. The rate constants for the 5-*exo* radical cation cyclizations apparently will be changed little in solvents of different polarity, but the rate constants for all of the other reactions are expected to vary as the solvent polarity changes. Specifically, one expects that an *increase* in solvent polarity will result in an increase in the rate constant for diffusive escape and a reduction in the relative rate constants for deprotonation or nucleophilic capture of the radical cation.

Fast cyclization of radical cation **1a** within the ion pair is almost certainly the reason that distonic radical cation product **6a** was detected in 15% yield when radical **5a-P** was allowed to react in THF. That is, ion pair escape in this low polarity solvent is not expected to be efficient. For example, we previously observed that a highly stabilized *p*-methoxystyrene radical cation produced by a β-phosphate heterolysis reaction did not give a diffusively free species in THF, although it did in polar solvents including ACN.[23] From the results for **1a** produced from **5a-P** in ACN, we estimated that the cyclization was about 5 times as fast as deprotonation or collapse to radical **24**, but in THF the cyclization reaction apparently is only 1/6 as fast as deprotonation or collapse to **24**.

If the rate constant for the cyclization has little or no solvent polarity effect in THF as is the case for the reactions in ACN and ACN containing TFE, the 30-fold change in relative rate constants upon proceeding from ACN to THF reflects a strong acceleration of the deprotonation and/or ion pair collapse reactions as the solvent polarity was decreased, consistent with the generalizations made above. That is, poorer solvation enhanced nucleophilicity and/or basicity of the phosphate. Extending the crude kinetic approximations made for reactions in ACN to the reaction in THF, we estimate that the ion pair collapse and/or deprotonation reaction has a rate constant at ambient temperature of ca. $3-6 \times 10^{10}$ s^{-1}.

Thus, in ACN the ion pair has a lifetime on the order of 1 ns, but in the less polar solvent THF, the ion pair lifetime is reduced to ca. 20 ps. These values are important for mechanistic understanding and synthetic applications of radical cation reactions that employ radical heterolyses as the entries. Many synthetic applications of radical reactions involve the use of tin hydride and are conducted in low polarity solvents such as benzene or toluene. In these solvents, one should not expect that diffusively free radical cations would be produced from β-phosphate radicals. Conversely, the production of diffusively free radical cations from heterolyses of C4′ DNA radicals and their models in water is expected to be quite efficient.

Measured Kinetics of Heterolysis Reactions. The "heterolysis reaction" is composed of multiple processes, the heterolysis step that gives a contact ion pair, possibly equilibration of a contact ion pair with a solvent-separated ion pair, and diffusive escape from the ion pair (Scheme 7). Different experimental methods might measure different steps in the heterolysis reaction, and that appears to be the case for various studies of β-phosphate radicals.

Scheme 7

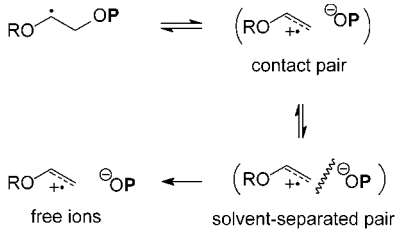

In our previously reported intermolecular approach for measuring heterolysis of radicals **19**, the technique provided rate constants for formation of diffusively free radical cations.[9] If equilibrations of the radical-cation−anion pairs with the β-phosphate radicals occur in the systems studied here, then the rate constants for heterolysis of radicals **5a-E** and **8a** will be greater than those found when diffusively free radical cations are formed because radical cations **1a** and **2a** cyclize partially within the ion pair. This equilibration effect might explain why the rate constants for heterolysis of **5a-E** and **8a** are apparently orders of magnitude greater than those for heterolysis of radical **19-E**.

A different situation was encountered when Gugger et al. studied the rate of heterolysis of radical **20**.[19] In that work, the method involved competition between trapping **20** by PhSH and formation of the radical cation that eventually reacted with the solvent, methanol.[19] The polarity of MeOH as evaluated on the $E_T(30)$ solvent polarity scale (55.4)[35] is greater than that for ACN (45.6)[35] and for solutions of 0.5% TFE in ACN (determined here as $E_T(30) = 52$). Therefore, the heterolysis reactions of **5a-E** and **8a** in MeOH should be somewhat faster than we can measure with our technique. Nonetheless, the rate constant for heterolysis determined for **20** ($k > 3 \times 10^9$ s^{-1}) appears to be almost an order of magnitude faster than what might be expected for **5a-E** and **8a** in the same solvent if a linear correlation between log k and $E_T(30)$ exists as found in other radical heterolyses.[23] It is interesting to speculate that the apparent fast heterolysis of radical **20** might involve a favorable stereoelectronic effect that is enforced by the structure of the radical such that the entropy of activation for the heterolysis is considerably reduced from that observed with **5a-E** and **8a**.

An Enol Ether Radical Cation Kinetic Scale. As we demonstrated with water and MeOH trapping, the reporter LFP method can be used for direct determinations of rate constants for reactions of enol ether radical cation **1c**. These types of LFP studies can be performed with a wide range to nucleophiles, bases, and reductants to establish a kinetic scale for enol ether radical cations that would be useful for mechanistic understanding and in the design of synthetic applications. We caution, however, that radical cation **1c** is not an optimal system for these kinetic studies. The inherent cyclization reaction is slow enough such that bimolecular reactions leading to decay complicate the measurements. The 6-*exo* cyclizations of **1b** and

(32) Johnson, C. C.; Horner, J. H.; Tronche, C.; Newcomb, M. *J. Am. Chem. Soc.* **1995**, *117*, 1684−1687.
(33) Horner, J. H.; Martinez, F. N.; Musa, O. M.; Newcomb, M.; Shahin, H. E. *J. Am. Chem. Soc.* **1995**, *117*, 11124−11133.
(34) Musa, O. M.; Horner, J. H.; Shahin, H.; Newcomb, M. *J. Am. Chem. Soc.* **1996**, *118*, 3862−3868.
(35) Reichardt, C. *Chem. Rev.* **1994**, *94*, 2319−2358.

2b, with rate constants of about 3×10^7 s^{-1} at ambient temperatures, are not useful for these types of measurements because they are too fast. An optimal unimolecular reaction for LFP studies probably would have a rate constant of about 1×10^6 s^{-1} at ambient temperature.

Conclusion

The unimolecular reporter method for studies of enol ether radical cations and their progenitor radicals developed here provides both kinetic and mechanistic insights. The reactions are complex, and one observes strong solvent polarity effects in the formation of diffusively free radical cations from radical heterolyses. The radical reactions of the radical cations, such as the cyclizations we studied, are highly accelerated, whereas the cation reactions, such as trapping with water, are greatly retarded. These characteristics can be employed advantageously in synthesis because a radical-type reaction of the radical cation gives either a distonic radical cation or a radical plus a cation product, and the reactivities of the products will be diminished for the radical and enhanced for the cation. Thus, it is likely that cascade synthetic conversions involving enol ether radical cations will be useful. We expect that applications of these intermediates will increase when kinetic scales are available and mechanistic understanding is improved.

Experimental Section

Syntheses. The synthetic work is described in the Supporting Information. Intermediate products typically were characterized by NMR spectroscopy and HRMS. The PTOC esters are thermally unstable and were characterized by NMR spectroscopy and, in some cases, electrospray HRMS.

Laser Flash Photolysis. Acetonitrile (HPLC grade) used in LFP studies was purchased from Fisher and used as received. 2,2,2-Triflouroethanol was stirred over $CaSO_4$ and $NaHCO_3$, filtered, and distilled. LFP studies were performed with an Applied Photophysics LKS-50 kinetic spectrometer using a Nd:YAG laser at 355 nm. Solutions of the PTOC precursor having an absorbance of 0.2 to 0.5 at 355 nm were placed in a thermally jacketed addition funnel and sparged with helium. The temperature of the solution was adjusted by circulation of a water/ethylene glycol solution from a regulated bath through the jacket. The solutions were allowed to flow through a quartz cell (1 cm $\times$ 1 cm i.d.). Temperatures were measured with a thin wire copper/Constantan thermocouple placed in the flowing stream immediately above the irradiation region of the flow cell. For measurements below 10 °C, the addition funnel and flow cell were placed in a nitrogen-purged box fitted with quartz windows.

Kinetic Data Analyses. For kinetic runs, several traces typically were averaged to improve signal-to-noise. Fitting the experimental data to a first-order exponential growth using nonlinear least-squares methods was performed with Applied Photophysics software. The analysis of consecutive reactions (radical **8b** in ACN) was performed with Sigmaplot.[36]

Acknowledgment. We are grateful to the NSF (CHE-0296027) for financial support.

Supporting Information Available: Synthetic details and tables of kinetic data (PDF). This material is available free of charge via the Internet at http://pubs.acs.org.

JA0177399

(36) *Sigmaplot*, ver. 2.0; Jandel Scientific Software: San Rafael, CA, 1994.